2

Phase-stable molecular phase modulation

Contact p.bustard1@physics.ox.ac.uk

P. J. Bustard[1], B. J. Sussman[1,2] and I. A. Walmsley[1]

[1] *Clarendon Laboratory, University of Oxford, Parks Road, Oxford OX1 3PU, UK*

[2] *Steacie Institute for Molecular Sciences, National Research Council of Canada, 100 Sussex Drive, Ottawa, Ontario, Canada K1A 0R6*

Introduction

Control and investigation of material dynamics on ever shorter timescales has been made possible by the development of ultrashort laser pulses into the few-femtosecond and attosecond regime. One of the most exciting areas of research has been in the use of molecular phase modulation (MPM) to synthesize and modify few-fs pulses [1,2,3,4]. All such MPM techniques use the rapid variation in electric susceptibility due to coherent molecular rotational or vibrational motion to generate new frequencies by phase modulation of pump or probe radiation.

Isolated few-fs pulses have been generated by impulsively driving molecular motion using high energy pulses and then scattering a probe pulse from the decaying excitation [2,3]. This approach requires high energy ultrashort pump pulses. In contrast, broadband combs of Raman sidebands have been generated by adiabatically exciting a high vibrational coherence in deuterium using two ns-duration pump pulses; such sidebands have been used to synthesize long trains of closely spaced, few-fs pulses [1,5]. In this technique the length of the fs pulses within the train varies from shot to shot. More recently, full interpulse phase-locking has been achieved by using a single ns-pulse and its second harmonic as pump pulses [6].

In this article we propose a new technique for the generation of isolated ultrashort pulses: ultrafast molecular phase modulation of a femtosecond probe pulse in rotating (or vibrating) molecules, with phase control of the molecular dynamics by impulsive stimulated Raman scattering (ISRS). We present the basic principles of the new technique and experimentally study the necessary conditions for its implementation.

The Scheme

The schematic diagram in Figure 1 illustrates the basic principles of the experiment. There are three main stages to the proposed scheme. Firstly, a small molecular coherence with a well defined phase is generated by ISRS using a small fraction of the femtosecond pulse energy, hereafter referred to as the seed. For impulsive excitation, this pulse must have a duration $\tau_{seed} < T_{osc} = 2\pi/\Omega = 2Bc(2J + 3)$ where Ω is the Raman frequency shift associated with the molecular oscillations, B is the rotational constant, c is the speed of light and J is the rotational quantum number. In the frequency domain this means that the pulse bandwidth covers both rotational levels, with frequency pairs satisfying the Raman resonance condition, and will generate optical phonons (delocalized rotational quanta). In the second stage, a longer, phase independent, pump pulse with duration τ_{pump} satisfying $\tau_{pump} \gtrsim T_2$ where T_2 is the damping time of the molecular coherence, generates a large rotational coherence by stimulated Raman scattering. In an unseeded gas, such a pump pulse will generate a Stokes field and rotational coherence with a random phase due to initiation by spontaneous Raman scattering. However, when the medium is seeded by ISRS, the resulting material excitation stimulates emission from the pump field ω_L to the Stokes field $\omega_S = \omega_L - \Omega$, and in the process more molecules are excited with the same phase as the seed excitation.

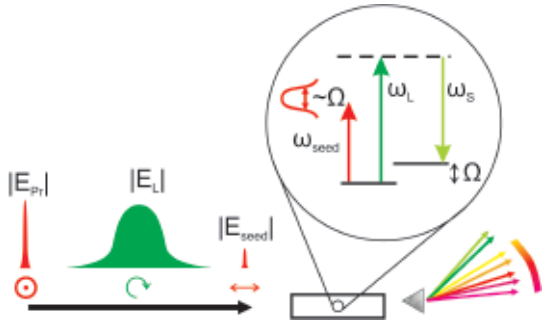

Figure 1. Schematic diagram of proposed pulse sequence.

In the second stage, a longer, phase independent, pump pulse with duration τ_{pump} satisfying $\tau_{pump} \lesssim T_2$ where T_2 is the damping time of the molecular coherence, amplifies the weak excitation by stimulated Raman scattering. Normally, such a pulse will generate a Stokes field with a random phase due to initiation by spontaneous Raman scattering. This occurs because the first stage material excitation stimulates emission from the pump field ω_L to the Stokes field $\omega_S = \omega_L - \Omega$, and in the process more molecules are excited with the same phase as the initial excitation. Macroscopically, this amplified molecular motion results in a rapidly varying electronic susceptibility, with a phase set by the initial seed pulse. In the final stage, the remaining probe pulse is spectrally

Figure 2. Schematic diagram of molecular alignment setup. Pr: probe; GT: Glan-Thompson polarizer; DC: Dichroic mirror; BF: Schott glass filter (BG37); PMT: Photomultiplier tube detector.

broadened by MPM on propagation through the excited molecules. If the probe pulse satisfies $\tau_{probe} < T_{osc}$, it will be continuously redshifted and/or blueshifted, depending on its delay time relative to the molecular motion.

Experiments

We use a 2 kHz chirped pulse amplifier (CPA) Ti:Sapph laser system generating tseed ~55 fs pulses centered at 800 nm as a source of seed and probe pulses. Pump pulses are generated by a 10 Hz frequency doubled Nd:YAG laser system with a pulse duration τ_L ~10 ns, running in an unseeded configuration. The gas sample was contained in a 30 cm cell with pressures from 0.5 bar to 7 bar. Hydrogen (H_2) gas was used because of its relatively high Raman gain, and rapid rotational period (T_{osc} = 56.97 fs for ortho-H_2). All beams were collimated to a $1/e^2$ intensity beamwaist ω_0 ~ 3 mm focussed into the cell using a 30 cm achromatic lens. Two experimental arrangements were used.

Impulsive alignment

The scheme described above relies on the ability to impulsively excite a molecular coherence using an ultrashort pulse. This section describes a transient molecular alignment experiment to demonstrate the impulsive excitation of a rotational coherence.

In the impulsive alignment setup, an ~50 μJ, ~55 fs, 800 nm seed pulse, linearly polarized at 45° to the bench aligns the molecules by ISRS. The molecules subsequently rotate freely in space, with transient alignment revivals when the excited rotational wavepacket rephases at time intervals $(Bc)^{-1}$. During the transient alignment revivals, the gas sample is birefringent due to the anisotropic molecular polarizability. We probe the decaying transient birefringence as a function of seed-probe time decay τ_{decay} using a 400 nm probe pulse propagating through crossed polarizers arranged at either end of the gas cell. In this Kerr cell arrangement, the first polarizer transmits vertically polarized light; the second transmits horizontally polarized light. Probe light, rotated from vertical to horizontal polarization by the molecular birefringence, is detected by a photomultiplier tube (PMT). The pump radiation is removed using a spectral filter before the PMT.

Measurements of the vertically polarized 400 nm light indicate that the seed pulse is sufficiently short and intense to transiently align some of the molecular sample, making it birefringent. Initial scans in N_2 show a rich structure of molecular alignment revivals, decaying with seed-probe delay (see Fig. 3, top). The scans in H_2 again show a decaying birefringence signal, however no beating or revival structure is evident, due to limited temporal resolution (see Fig. 3, bottom).

The birefringence signals are signatures that the seed pulse is impulsively exciting a coherent superposition of rotational levels. The qualitative difference between N_2 and H_2 is due to the different energy spacing of their rotational levels $\omega_J = 2\pi cBJ(J+1)$. Hydrogen has a much larger rotational level spacing than nitrogen ($B(H_2)$ = 60.853 cm^{-1}; $B(N_2)$ = 1.998 cm^{-1} [7]). This has two main consequences for the alignment experiment. Firstly, at room temperature the N_2 population is distributed over dozens of rotational levels, while ~65% of the H_2 population is in the (v = 0, J = 1) level, with the rest in the other low-J states. Secondly, due to the relatively large frequency spacing of rotational levels in H_2, the seed pulse only has sufficient bandwidth to impulsively excite two-photon Raman transitions among the lowest J-levels. In contrast, the smaller rotational spacing in N_2 means that the seed can impulsively excite transitions among many more J-levels. As a result, in N_2 the birefringence signal consists of sharp peaks spaced by $(Bc)^{-1}$ due to the interference of many $J' \longleftrightarrow J''$ coherences. In H_2 the seed bandwidth limits coherences to only 4 levels, and the narrow population spread means that the $J' = 1 \longleftrightarrow J'' = 3$ transitions should dominate the signal. The birefringence signal is expected to vary with period equal to the molecular rotational period, T_{rot} = 56.83 fs. We do not observe these oscillations because the 400 nm probe pulse is not sufficiently short to resolve the molecular motion.

Amplification

In this section we present three main results. Firstly, we compare the efficiency of the first pump-rotational Stokes sideband (RS1) generation in seeded and unseeded H_2. Secondly, we find the optimal seed-pump delay for RS1 generation in our setup. Optimization of the RS1 signal is a simple way of maximizing the generation of coherent rotational quanta because for each RS1 photon created, a single rotational quantum is also created. Finally, we demonstrate that the rotational motion generated by the SRS process is strong enough to spectrally broaden probe pulses.

In the amplification setup, linearly polarized 55 fs, 800 nm pulses, are used to either seed or probe the gas

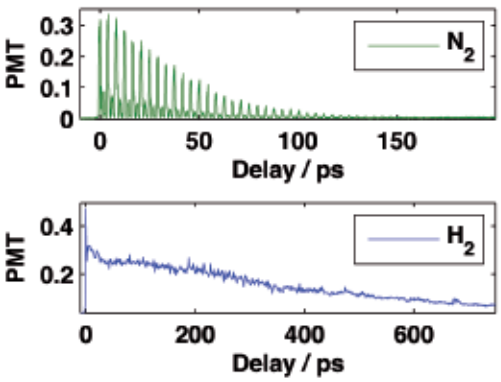

Figure 3. Plot of photomultiplier tube (PMT) signals measuring transient birefringence in N_2 at 2.3 bar (top) and H_2 at 4.1 bar (bottom). The decay is due to collisional dephasing. Note the different abscissa scales.

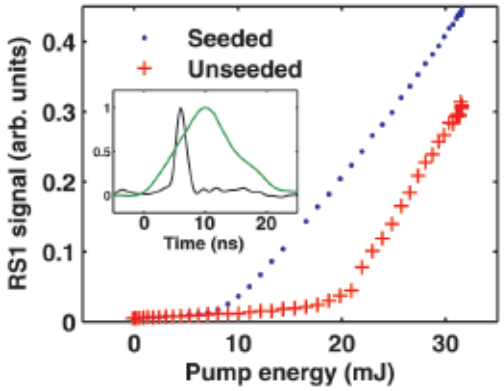

Figure 4. Pump rotational Stokes 1 sideband energy as a function of pump energy for a seeded (blue) and unseeded (red) cases. The insert shows the relative delay of the seed pulse (black) and the pump pulse (green) as measured by a photodiode ($\tau_{response} \approx 1$ ns).

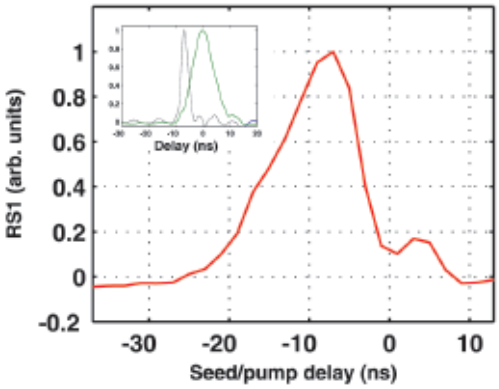

Figure 5. Plot of RS1 energy (red trace) as a function of seed-pump delay. The inset shows the relative photodiode traces of the seed (blue) and pump (green) pulses for the optimal delay. The small increase in the signal between 0-10 ns is due to excitation by satellite pulses from the CPA.

sample. Circularly polarized 532 nm pump pulses are used to create coherent rotational motion by generating a Stokes field at 550 nm (RS1) by stimulated Raman scattering (SRS). In the seeding experiments, the SRS process is initiated by the excitation generated by the ultrashort seed pulse while in the unseeded experiments, the excitation is initiated by spontaneous quantum noise. The attenuated RS1 field is measured by a photodiode while the seed (or probe) pulse spectrum was measured using an Ocean Optics USB2000 spectrometer. The seed-pump delay was varied electronically using a Stanford delay generator.

Figure 4 shows the dependence of RS1 energy on the pump energy for both seeded and unseeded cases, at a gas pressure of 3.7 bar. The seed pulse was temporally overlapped with the rising edge of the pump pulse; the seed energy was 12.5 μ*J*. The seeded case is clearly more efficient than the unseeded case. In the unseeded case, the macroscopic RS1 field is initiated by spontaneous Raman scattering which stimulates further emission to the RS1 field. However, when the pump encounters a medium with an initial rotational excitation from seeding, the RS1 generation is more efficient because the amplitude of the initial rotational motion exceeds that of the quantum noise (which is one phonon per mode)[8].

Figure 5 shows the dependence of RS1 energy on the seed-pump delay and the seed energy for fixed pump energy 54 ± 2 mJ; the cell pressure was ≈ 0.5 bar giving $T_2 \approx 6.2$ ns[9], where T_2 is the Raman dephasing time. For the parameters used in this plot, the RS1 sideband was below the detection threshold when the seed pulse did not arrive before or during the pump pulse envelope. Figure 5 shows that the optimal RS1 generation, by extension the optimal phonon generation, occurs when the seed pulse immediately preceeds the pump pulse. This is explained by a simple consideration of the causal nature of the interaction. At earlier seed arrival times, the excitation generated by the seed decays due to collisional dephasing before the pump arrives and so the SRS amplification process is less efficient. When the seed and pump overlap, the amplification process is again sub-optimal because the front part of the pump propagates in an unseeded medium, making it unable to contribute to the coherent amplification process. However, if the seed arrives immediately before the pump pulse, less collisional dephasing occurs and the majority of the pump energy is used to amplify the molecular coherence, making the amplification most efficient.

Figure 6 shows the spectrum of a probe pulse when temporally delayed relative to the seed pulse by $\tau_{delay} = 3.87$ ns; the pump energy was 60 ± 2 mJ. The continuous spectral broadening in Figure 6 demonstrates that the pump pulse creates a molecular rotational coherence capable of significant MPM of probe radiation. Simulations indicate that the modulation efficiency could be increased by improving the phase-matching between the group velocity of the probe radiation and the phase velocity of the Raman excitation. Attractive candidates for improved phase-matching include gas filled hollow-core capillaries or photonic crystal fibres.

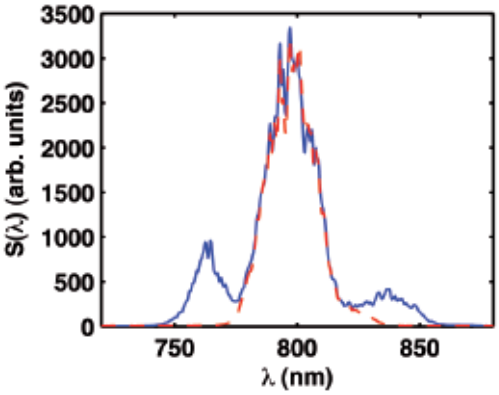

Figure 6. Plot of normalized probe spectrum before (dashed, red trace) and after (blue trace) molecular phase modulation by rapidly rotating H_2 molecules. The SRS process was initiated by ISRS using a seed pulse; the cell pressure was 2 bar; the pump energy was 60 mJ; the seed-probe delay was $\tau_{delay} = 3.87$ ns.

Conclusion and future work

We have demonstrated impulsive molecular alignment of H_2 and N_2 molecules as a means of seeding a molecular coherence. The rotational coherence in H_2 was subsequently amplified by stimulated Raman scattering. This coherent rotational motion is capable of generating significant spectral broadening of a separate probe pulse and offers the exciting prospect of an efficient, phase stabilized molecular phase modulator. Future work will involve improving the modulation efficiency to generate larger bandwidths and demonstrating seed-probe delay modulation.

Acknowledgements

The authors gratefully acknowledge support from the Rutherford Appleton Laboratory Laser Loan Pool. This work was funded in part by the Research Councils UK as part of the Basic Technology program, under the aegis of the UK Attoscience Consortium. B.J.S. gratefully acknowledges support from the Natural Sciences and Engineering Research Council of Canada, and from The Royal Society.

References

1. A. V. Sokolov and S. E. Harris. Ultrashort pulse generation by molecular modulation. *J. Opt. B: Quantum Semiclass.*, **5**:R1 (2003).
2. N. Zhavoronkov and G. Korn. Generation of single intense short optical pulses by ultrafast molecular phase modulation. *Phys. Rev. Lett.*, **88**:203901-1 (2002).
3. R. A. Bartels, T. C. Weinacht, N. Wagner, M. Baertschy, C. H. Greene, M. M. Murnane and H. C. Kapteyn. Phase modulation of ultrashort light pulses using molecular rotational wave packets. *Phys. Rev. Lett.*, **88**(1):013903 (2001).
4. M. Spanner and M. Y. Ivanov. Optimal generation of single-dispersion precompensated 1-fs pulses by molecular phase modulation. *Opt. Lett.*, **28**(7):576-578 (2003).
5. M. Y. Shverdin, D. R. Walker, D. D. Yavuz, G. Y. Yin and S. E. Harris. Generation of a single-cycle optical pulse. *Phys. Rev. Lett.*, **94**(3):033904 (2005).
6. Z-M. Hsieh, C-J. Lai, H-S. Chan, S-Y. Wu, C-K. Lee, W-J. Chen, C-L. Pan, F-G. Yee and A. H. Kung. Controlling the carrier-envelope phase of Raman-generated periodic waveforms. *Phys. Rev. Lett.*, **102**(21):213902 (2009).
7. G. Huber and K. P. Herzberg. *Molecular Spectra and Molecular Structure. IV. Constants of Diatomic Molecules*. Van Nostrand Reinhold Co., 1979.
8. M. Raymer and I. A. Walmsley. Quantum coherence properties of stimulated Raman scattering. *Progress in Optics*, **28**:181 (1990).
9. R. A. J. Keijser, J. R. Lombardi, K. D. Van den Hout, B. C. Sanctuary and H. F. P. Knaap. The pressure broadening of the rotational Raman lines of hydrogen isotopes. *Physica*, **76**(3):585-608 (1974).